In Vivo Evaluation of Electrospun Polycaprolactone Graft for Anterior Cruciate Ligament Engineering

Frank A. Petrigliano, MD,[1,*] Gabriel A. Arom, BS, MSc,[1,2,*] Azadeh N. Nazemi,[2]
Michael G. Yeranosian, MD,[1] Benjamin M. Wu, DDS, PhD,[2] and David R. McAllister, MD[1,3]

The anterior cruciate ligament (ACL) is critical for the structural stability of the knee and its injury often requires surgical intervention. Because current reconstruction methods using autograft or allograft tissue suffer from donor-site morbidity and limited supply, there has been emerging interest in the use of bioengineered materials as a platform for ligament reconstruction. Here, we report the use of electrospun polycaprolactone (PCL) scaffolds as a candidate platform for ACL reconstruction in an *in vivo* rodent model. Electrospun PCL was fabricated and laser cut to facilitate induction of cells and collagen deposition and used to reconstruct the rat ACL. Histological analysis at 2, 6, and 12 weeks postimplantation revealed biological integration, minimal immune response, and the gradual infiltration of collagen in both the bone tunnel and intra-articular regions of the scaffold. Biomechanical testing demonstrated that the PCL graft failure load and stiffness at 12 weeks postimplantation (13.27 ± 4.20N, 15.98 ± 5.03 N/mm) increased compared to time zero testing (3.95 ± 0.33N, 1.95 ± 0.35 N/mm). Taken together, these results suggest that electrospun PCL serves as a biocompatible graft for ACL reconstruction with the capacity to facilitate collagen deposition.

Introduction

RUPTURE OF THE ANTERIOR cruciate ligament (ACL) is a common orthopedic injury, with more than 200,000 cases presenting annually in the United States alone.[1] Due to limited vascularization of ligament tissue and the hostile environment of the intra-articular (IA) space, a ruptured ACL has little capacity for endogenous healing. Consequently, greater than 85% of ACL disruptions require surgical reconstruction.[1] Current reconstruction strategies employ autograft or allograft tendon or ligament tissues. Although subjective success rates of greater than 90% can be achieved with both autograft and allograft replacement, serious complications are associated with these reconstruction options.[2] Procurement of autograft tissue is associated with donor-site morbidity, including weakness, decreased range-of-motion, and chronic knee pain. Conversely, the use of allograft tissue increases the risk of pathogen transmission and adverse inflammatory response. Moreover, the supply of allograft tissue is limited by a finite donor pool.[3] Synthetic nondegradable grafts were developed in the 1970s and 1980s, but were hampered by premature graft rupture, foreign body reactions, osteolysis, and synovitis.[4] Accordingly, the development of alternative graft sources for ACL reconstruction has been the focus of recent efforts in the field of connective tissue engineering.

Polycaprolactone (PCL) is a biodegradable polymer that is Food and Drug Administration (FDA) approved for a number of medical applications, including adhesion barrier and wound dressing.[5] In a semicrystalline polymer, its crystallinity tends to decrease with increasing molecular weight. The good solubility of PCL, its low melting point (59–64°C), and exceptional blend compatibility has prompted extensive research into its potential application in tissue engineering.[6,7] PCL possesses superior rheological and viscoelastic properties over other resorbable polymers that render it easy to manufacture and manipulate into a large range of scaffolds.[7–13] Furthermore, the fact that a number of drug-delivery devices fabricated with PCL already have FDA approval and the CE Mark registration enables regulatory approval.[6] PCL has been used in a wide variety of applications, including vascular, bone, cartilage, nerve, skin, and esophageal tissue engineering.[3,10,11,14–19] While it has been studied as a braiding material for mixed polymer matrices, PCL has not been fully evaluated as a standalone candidate biomaterial for ligament engineering *in vivo*.[20] However, recent work by Hu *et al.* has demonstrated the potential feasibility of unblended PCL as a polymer for reinforcing tendon repair.[9]

Electrospinning is a relatively inexpensive technique for submicron and micron diameter fibers from polymer solutions. Electrospinning is of great interest as the resulting fiber diameters are in the size range (submicron to nanometer) of

[1]Department of Orthopaedic Surgery, David Geffen School of Medicine at University of California at Los Angeles, Los Angeles, California.
[2]Department of Bioengineering, University of California at Los Angeles, Los Angeles, California.
[3]Department of Surgery, Greater Los Angeles Veterans Administration Medical Center, Los Angeles, California.
*Cofirst authors.

the extracellular matrix microstructures, particularly the higher ordered collagen microfibrils.[6,13] The flexibility of the electrospun fibers, due to the very high aspect ratio (length/diameter), is also beneficial, allowing seeded cells to remodel their surrounding environment. Many research papers have focused on different natural and synthetic polymers, but PCL is one of the most commonly used polymers in the electrospinning literature.[6] Accordingly, electrospun PCL has been proposed for the engineering of ligament and tendon. In a recent *in vitro* rabbit model of Achilles' tendon repair, An *et al.* demonstrated that PCL microfibers were able to support the proliferation of human dermal fibroblasts over 7 days and that the microfibers were highly infiltrated by tendon tissue as early as 1 month.[21]

In light of the excellent biocompatibility, excellent mechanical strength, and appropriate degradation rate of PCL, we chose to utilize an electrospun PCL scaffold for the current experiment. We hypothesize that an electrospun PCL graft would promote collagen deposition and elicit minimal immunogenic response in an IA rodent model of ACL reconstruction. Furthermore, we hypothesized that maturation of the graft would result in improved biomechanical properties over time.

Materials and Methods

Scaffold fabrication

Medical-grade ester-terminated PCL in granule form (MW = 110,000; Lactel Absorbable Polymers, Birmingham, AL) was dissolved 10% w/w in 1,1,1,3,3,3-hexafluoro-2-propanol (Sigma-Aldrich, St. Louis, MO). The solution was electrospun around a lathe mandrel rotating at a speed of 3450 rpm, using a 20 kV voltage source and a constant infusion rate of 2.5 mL/h for a total of 0.5 mL per scaffold. Scaffolds were laser cut using a VersaLaser Cutter 2.3 (Scottsdale, AZ) and their microstructure characterized using a Nova NanoSEM 230 scanning electron microscope (Nova, FEI Company, Tokyo, Japan) operated at low-vacuum setting, 10.0 keV landing voltage, 6.4 mm working distance, and a probe diameter of 3.0. Scaffolds were then plasma etched (Harrick Plasma PDC-001 Plasma Cleaner, Ithaca, NY) to induce hydrophilicity, bathed in 70% EtOH, and collagen coated using a 8:1:2.5 sterile solution of Purecol (Advanced Biomatrix, San Diego, CA), 10× phosphate-buffered saline (PBS), and 0.1 N NaOH diluted 1:9 in 1× PBS at 4°C. After a 24-h incubation at 37°C and 24 h of drying, six scaffold layers were then stacked and affixed to one another using 4-0 vicryl sutures. For all experiments, PCL sheets with dimensions of 1.5 mm × 35 mm × 150 µm were fabricated by high-voltage electrospinning and laser cut to yield a porous scaffold with 150 µm diameter holes at 15% pore area. Scanning electron microscopy was utilized to characterize the three-dimensional fibrous mesh and the regular spacing of the laser cut pores (Fig. 1A–C). Laser cut pores were employed because they have been shown to promote vascularization and infiltration of cells vital to tissue regeneration.[18] The scaffold sheets were arranged into a stacked conformation with six individual PCL sheets (Fig. 1D).

Animal model and operative reconstruction

An adaptation of a previously established rat ACL reconstruction model[22,23] was performed utilizing 300 g, 75-day-old
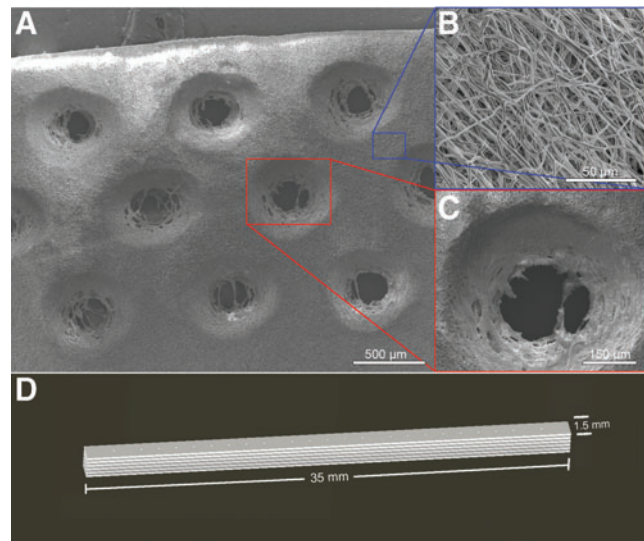
FIG. 1. Polycaprolactone (PCL) polymer design, fabrication, and three-dimensional rendering. PCL solution was electrospun and laser cut to yield a porous scaffold. **(A)** Low- and high-magnification scanning electron microscopy images show both **(B)** aligned fiber and **(C)** hole regions designed to facilitate cellular infiltration and collagen deposition in the scaffold. **(D)** Schematic of scaffold with dimensions of 1.5 mm × 35 mm × 900 µm and the eventual arrangement of the scaffolds into a stacked conformation. Color images available online at www.liebertpub.com/tea

Sprague-Dawley rats (Harlan Laboratories, Hayward, CA). The surgical procedure was performed on the lower left limb of the rat after induction of general anesthesia and surgical preparation. A midline incision was made over the knee and a medial parapatellar arthrotomy performed to expose the ACL, which was excised. The knee was flexed to ∼60° and a 1.4-mm Kirschner wire was used to drill the tibial and femoral tunnels, with care taken to include the tibial and femoral ACL footprints. Both sides of the grafts were affixed to a 1.2-mm Keith needle used to pass the graft through the bone tunnels (BT) across the joint space, replacing the native ACL. The ends of the graft were manually tensioned and secured to the periosteum and surrounding fascia of the distal part of the femur and proximal part of the tibia with 4-0 vicryl sutures. The wound site was closed in a layered manner. All animals were maintained pre- and postoperatively according to on-site protocol, and no complications related to surgery were noted.

At 2 and 6 weeks, animals ($n=4$) were sacrificed for histological analysis of biocompatibility and collagen deposition. At 12 weeks postimplantation, scaffolds underwent histological analysis ($n=4$) and standardized mechanical strength testing ($n=6$) (Fig. 2). Mechanical properties were compared to the native ACL of the contralateral limb in each animal ($n=6$). Furthermore, mechanical properties were compared to scaffolds that were implanted in age-matched (75-day) and weight-matched (300 g) controls and immediately sacrificed to provide a time-zero comparison ($n=6$). These time points were selected as they correspond to previous *in vivo* studies evaluating graft incorporation and were thought to provide longitudinal evaluation of the early (2 weeks), intermediate (6 weeks), and late (12 weeks) incorporation of the PCL graft in the rodent knee.[22]
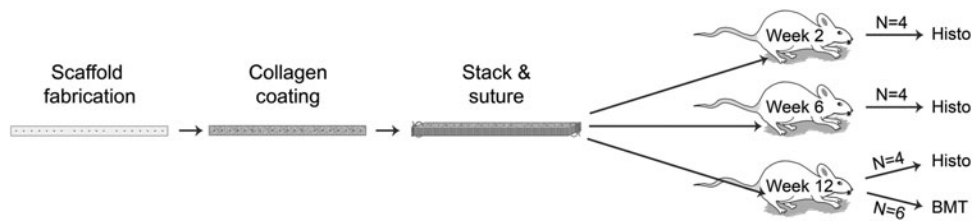
FIG. 2. Schematic demonstrates *in vivo* experimental design. Scaffolds are prepared, stacked, and coated with collagen before implantation into the left knee of model rodents. Replicates are designed such that four animals will be assessed for biological function at weeks 2, 6, and 12 postimplantation, and an additional six will undergo biomechanical testing (BMT) at week 12.

Histological analysis and immunohistochemistry

For immunohistological analysis, the left knee of each animal was fixed in 10% formalin at 25°C for 72 h. Fixed knee harvests were submitted to a core laboratory for decalcification, sectioning, mounting, hematoxylin and eosin (H&E) staining, and slide digitization. Immunofluorescent staining was used to detect the presence of (1) cells of macrophage lineage using a mouse anti-rat CD68 antibody and (2) collagen using a rabbit anti-rat type 1 collagen antibody (Millipore, Billerica, MA). Paraffin-embedded slides were dewaxed with two xylene washes at 5 min each, followed by 100%, 95%, and 75% ethanol baths at 2 min each. Rehydration was complete with a 2-min rinse in dH_2O, followed by boiling for 20 min in $1\times$ Citra AR Solution (Sigma-Aldrich) for antigen retrieval. Sections were permeabilized in a 0.025% Triton X wash (Sigma-Aldrich) and blocked at 25°C for 1 h in a TBS Tween-20X solution of 4% normal goat serum and 0.4% bovine serum albumin. Sections were incubated overnight at 4°C with 1:100 dilution of the primary antibody in a blocking solution, followed by a 30-min incubation at room temperature with 1:500 dilution of fluorescent secondary antibody: (1) Alexa Fluor 488 goat anti-mouse for CD68 and (2) Alexa Fluor 633 goat anti-rabbit for type I collagen (Invitrogen, Grand Island, NY). Slides were mounted with DAPI-Prolong Gold (Life Technologies, Eugene, OR) and imaged using a Nikon Instruments Eclipse Ti Inverted Microscope System (Irvine, CA).

Analysis of collagen deposition

Visualization of fibrillar types I and III collagen was performed using the Picrosirius Red Stain Kit (Polysciences, Inc., Warrington, PA) after deparaffinization and imaged under polarized light using a DMLB Leica Microscope (McBain Systems, Chatsworth, CA). Images were taken at $40\times$ objective magnification to ensure that the field of view included the scaffold, but no surrounding tissue. Images were analyzed for area fraction of collagen by measuring the number of birefringent pixels relative to total using ImageJ software ($n=5$) (National Institutes of Health, Bethesda, MD).

Histological grading

Digitized section images were analyzed using a modified histological grading scale previously reported in the literature.[24,25] Six parameters—cell morphology, inflammatory response, matrix staining intensity, fibrocartilage formation, new bone formation, and graft bonding to bone—were assigned categorical values (ranging 0–3, corresponding to none to abundant) to assess the biological integration of the grafts. Slides were graded by two, independent blinded evaluators. Individual scores were summed to give a composite score ranging from 0 to 6 per category per animal, and Cohen's kappa coefficient (κ) was computed to indicate inter-rater agreeability.[26]

Biomechanical testing

All soft tissues except the graft were removed from the harvested knees with the aid of a dissecting microscope. The femur and tibia were potted in polymethylmethacrylate with the knee in 90° flexion to prevent femoral epiphyseal separation during testing. The graft was kept moist during dissection and potting by regular and frequent spraying of PBS solution. The femur–graft–tibia complex was mounted onto an Instron tensile tester (Model 5564, Norwood, MA) with a 1 kN load cell. The graft was pretensioned to 2N and then tested to failure at a strain rate of 0.5 mm/s. The data were used to generate a load–displacement curve, and the peak and slope of the linear portion of the curve were used to determine failure load and stiffness, respectively, for three groups: (1) implanted grafts at 12 weeks postoperatively, (2) grafts immediately following implantation (time 0), and (3) native ACLs from age- and weight-matched rats ($n=6$).

Statistical analysis

For Picrosirius red staining and $CD68^+$ cell counts, five distinct images of the implanted scaffold were obtained in both the BT and IA regions. The mean and standard error of the mean were calculated, and a two-way ANOVA with Bonferroni correction was used to assess differences between time points and graft regions. Differences between time points were verified using unpaired t-tests. Significance was set at $p<0.05$. For histological grading that used categorical variables, agreement between individual raters was analyzed using Cohen's kappa coefficient (κ).

Results

Rodent ligament reconstruction model

The surgery was performed as previously described, and the graft imaged *in situ* (Fig. 3A). In all animals, the quality and orientation of the grafts were evaluated using H&E staining of tissue sections (Fig. 3B). Careful assessment of
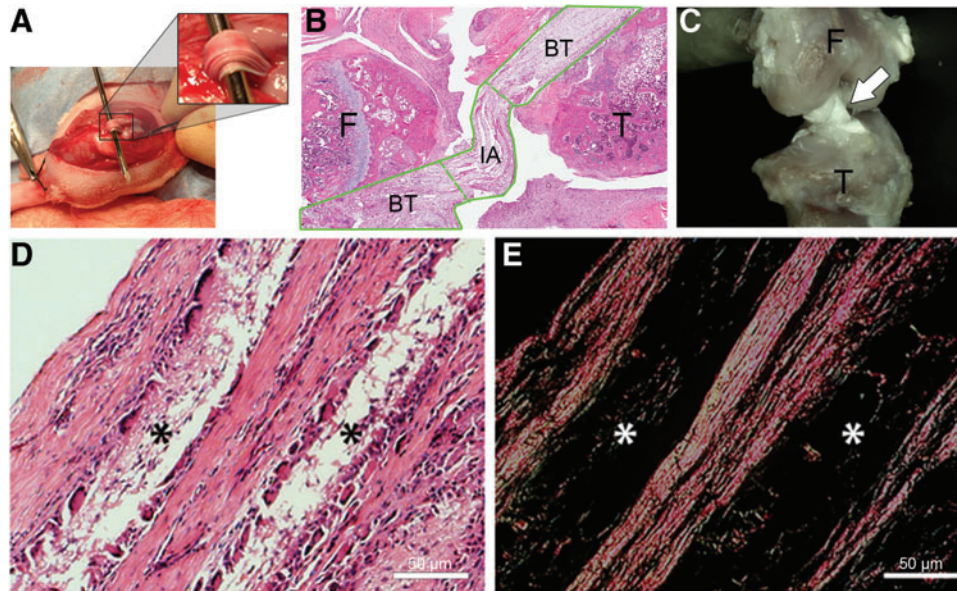
FIG. 3. Gross and histological images of PCL implant are shown **(A)** intra-operatively and postoperatively with **(B)** hematoxylin and eosin (H&E) staining and **(C)** digital photomicroscopy. Tibial and femoral tunnels were drilled in the native footprint of the anterior cruciate ligament (ACL). The graft is passed and fixed extra-articularly with sutures to the periosteum. Images of PCL graft harvested at 12 weeks postimplantation and stained with **(D)** H&E and **(E)** Picrosirius red reveal resorption of graft (*) and replacement with densely aligned collagen. BT, bone tunnel; IA, intra-articular; F, femur; T, tibia. Color images available online at www.liebertpub.com/tea

stained sections identified two functionally distinct regions of the graft: (1) BT regions where the graft was surrounded by tibial and femoral bone, and (2) an IA region within the knee joint that was comparable to the native ACL. In animals designated for mechanical testing, gross imaging using digital microscopy was used to verify integrity of the graft before testing (Fig. 3C). At 12 weeks following the reconstruction, histological analysis of the sectioned knee demonstrated that the scaffold matrix became largely infiltrated by fibroblasts secreting eosinophilic collagen and native immune cells (Fig. 3D). Picrosirius red staining demonstrated highly aligned collagen filling the spaces produced by the graft manufacturing procedure (Fig. 3E).

Biocompatibility of implanted PCL grafts and in vivo *collagen deposition*

To assess biocompatibility as measured through the local inflammatory response, histological analysis was performed at 2, 6, and 12 weeks. There was evidence of a modest host inflammatory response, largely seen as infiltrating macrophages and foreign body cells that peaked at week 6 and subsided thereafter (Fig. 4). To corroborate this biocompatibility finding, sections were labeled using immunofluorescence staining for expression of CD68 (or ED1), a glycoprotein specifically expressed on cells of the macrophage/monocyte lineage. Using fluorescence microscopy, the number of $CD68^+$ cells were counted in several high-power fields (HPF) ($n=5$) in both the BT and IA regions of the implanted scaffold (Fig. 5A). This analysis demonstrated an increase in $CD68^+$ cells in both the IA region and BTs from week 2 (IA $= 0.30 \pm 0.30$ cells/HPF, BT $= 4.57 \pm 0.83$ cells/HPF) to week 6 (IA $= 17.27 \pm 2.30$ cells/HPF, BT $= 16.60 \pm 3.19$ cells/HPF) ($p < 0.01$). There was a subsequent decrease in the number of these inflammatory cells from week 6 to 12 (IA $= 9.33 \pm 0.71$ cells/HPF, BT $= 9.36 \pm 1.125$ cells/HPF) ($p < 0.01$) (Fig. 5B).

To evaluate for *in vivo* collagen deposition on the PCL graft, sections were immunofluorescently labeled for expression of type I collagen (Fig. 6). The collagen signal appears brightest at week 12 for both BT and IA graft regions.

To quantify collagen deposition, sections were stained with Picrosirius red and imaged under polarized light to visualize both type I and type III collagen fibers (Fig. 7A). Using ImageJ to analyze pixel intensity, the percentage of total area covered by collagen was quantified in the reconstructed ligament (Fig. 7B). After 12 weeks, collagen encompassed 71% of the BT graft area and 23% of the IA graft area, compared to 98% in the native ACL ($p < 0.01$).

Finally, categorical histological grading was performed on these histological sections by two, independent blinded reviewers (Table 1). Inter-rater agreement ranged from fair to excellent according to the Landis and Koch guidelines of kappa-type statistics.[27] All histological scores, except inflammatory responses, increase between samples analyzed at weeks 2, 6, and 12, suggesting improved biological integration of the scaffold. Over time, the number of flattened fibroblasts and their eosinophilic matrix secretion increased. The reconstructed knee also showed evidence of fibrocartilage and new bone formation in the BT region.

Biomechanical analysis of PCL graft

To assess the mechanical function of the PCL graft, tensile testing was performed on native ACLs harvested from rats, as well as PCL scaffolds immediately following implantation (time 0) and 12 weeks after implantation. All

FIG. 4. Histology panel of PCL grafts stained with H&E at weeks 2, 6, and 12 post-implantation. Evidence of a modest host inflammatory response is visible beginning at week 2 in the BT and week 6 in the IA graft region. Aligned collagen and fibroblasts are present in the IA graft tissue beginning at week 6. BT, bone tunnel; IA, intra-articular regions, Fb, fibroblast; FBG, foreign body giant cell; M, macrophage. Color images available online at www.liebertpub.com/tea
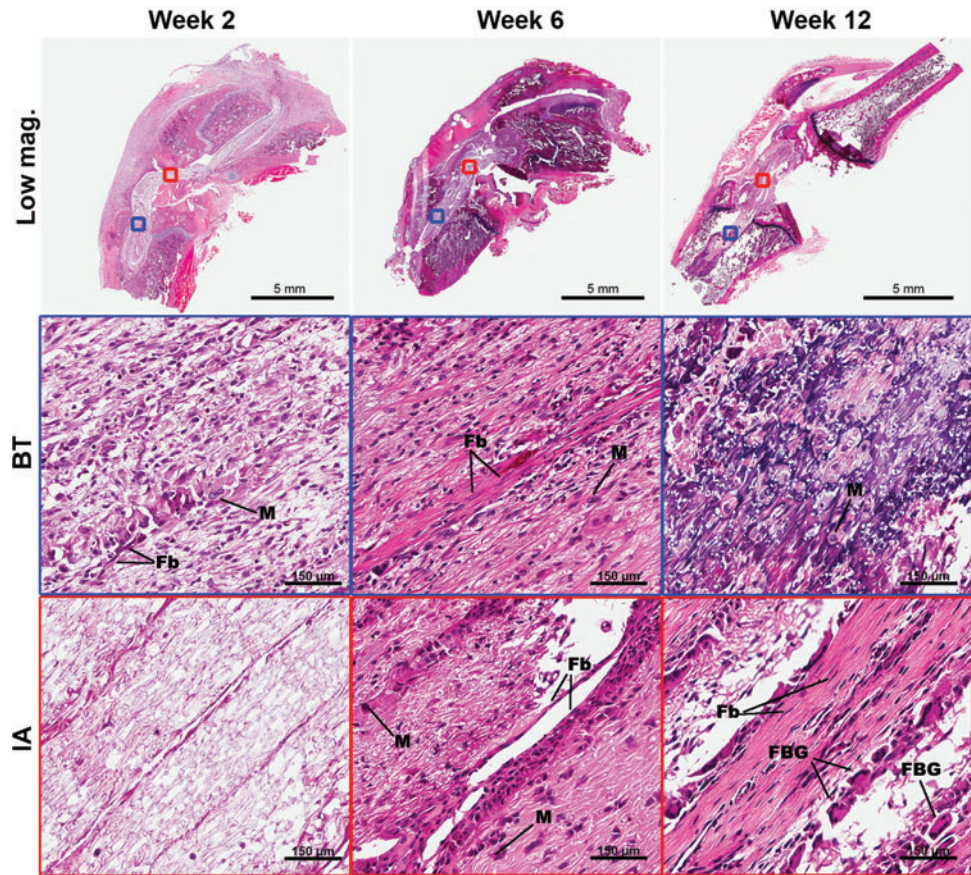
samples failed at the midsubstance during biomechanical testing. Using load–displacement curves generated from tensile testing, failure load and stiffness were computed for each substrate (Table 2). The mechanical properties of the graft following implantation (failure load $= 3.95 \pm 0.33$N, stiffness $= 1.95 \pm 0.35$ N/mm) increased significantly ($p < 0.01$) after 12 weeks *in vivo* (failure load $= 13.27 \pm 4.20$, stiffness $= 15.98 \pm 5.03$ N/mm).

Discussion

Previous studies of tissue-engineered ligament reconstruction have implanted braided or extruded grafts made of a variety of materials, including silk, PLLA, and polyurethane.[24,28–32] Although these materials resulted in successful integration of the graft, none was able to recapitulate the strength of the native ACL.[3,29,33–36] While many polymers,
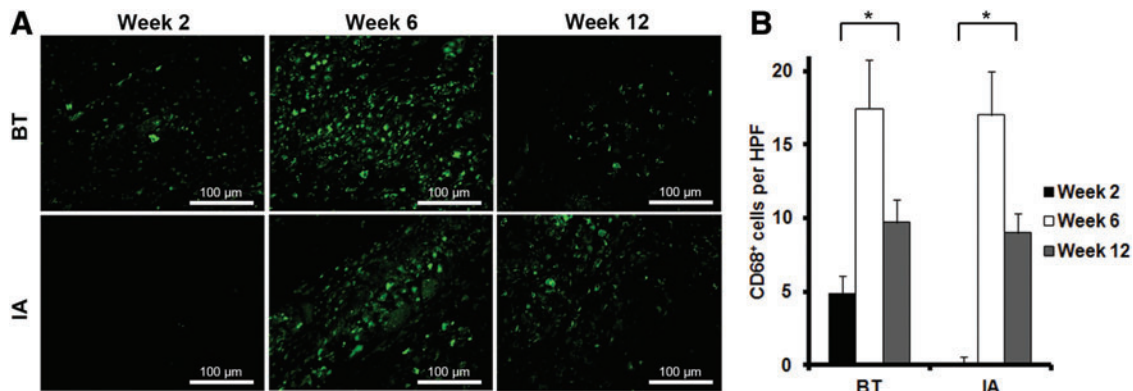
FIG. 5. Immunological staining and analysis of CD68 (ED1) macrophage lineage marker. **(A)** Graft sections were stained for expression of CD68 with representative images shown and **(B)** the number of CD68^{+} cells were counted in each high-power field ($n = 5$) (HPF, $40\times$ objective magnification) at 2, 6, and 12 weeks postimplantation, demonstrating that inflammatory responses peaked at 6 weeks postimplantation and decreased thereafter. *A p value of < 0.01 between all time points. Color images available online at www.liebertpub.com/tea
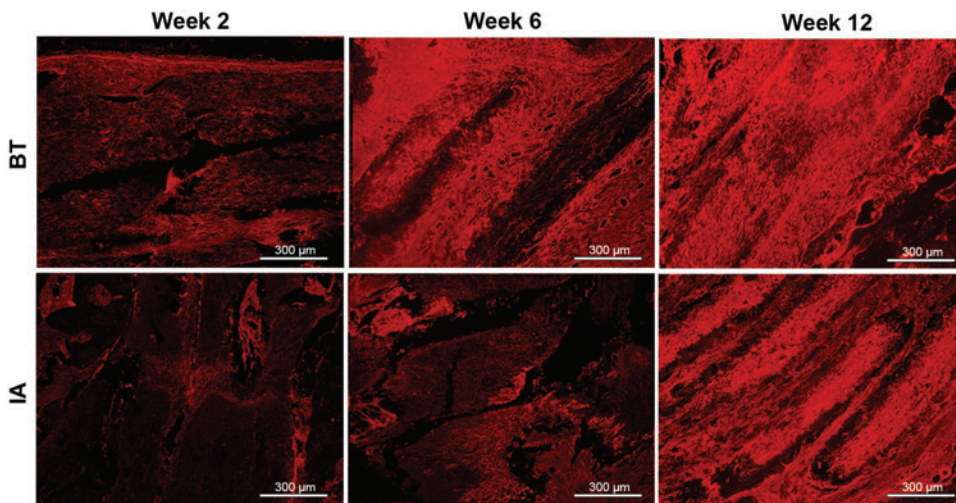
FIG. 6. Immunoflourescent staining of type 1 collagen was performed on graft samples harvested at weeks 2, 6, and 12 postimplantation demonstrated increased collagen deposition in the graft over time. Color images available online at www.liebertpub.com/tea

including polymer blends that incorporate PCL, have been proposed for use in ligament reconstruction, this study investigated standalone PCL as it is biologically inert, nontoxic, degrades slowly *in vivo*, and is easily synthesized and manufactured into a desired conformation.[37] PCL is also mechanically robust and shows little plastic deformation under mechanical stress.[38] Its use has been established in the bone tissue engineering literature as a reliable reservoir for mineralization and type I collagen deposition due to its aligned nanofiber structure when electrospun.[39] Furthermore, its standalone use has more recently been proposed for extra-articular tendon repair and replacement.[9] In the current study, we hypothesize that an electrospun PCL graft would promote collagen deposition and elicit minimal immunogenic response in an IA rodent model of ACL reconstruction and that maturation of the graft would result in improved biomechanical properties over time.

### Biocompatibility of implanted PCL grafts

The data from this study suggest that the PCL graft elicited a modest, transient immune response in the rodent knee. Macrophage infiltration was observed 2 weeks after implantation in the BT region only, peaked at 6 weeks in both graft regions, and began to subside after 12 weeks. The quantity of macrophages

found in this study is similar to that reported by Kawamura *et al.* after reconstruction of a rat ACL using an autologous tendon graft, the current gold standard for ACL reconstruction.[23] In addition, Kawamura *et al.* found that macrophages are crucial in the healing of the graft–bone interface.[23] Thus, the persistent macrophage infiltration present at 12 weeks in the implanted electrospun PCL graft and BT may reflect ongoing IA graft maturation and healing within the BT.

In vivo *collagen deposition on implanted PCL grafts*

Grafts were relatively devoid of collagen after 2 weeks postimplantation, as demonstrated by both type I collagen and Picrosirius red staining. After 2 weeks, the implanted graft demonstrated histological characteristics consistent with the inflammatory phase of neoligamentization, while robust cellular proliferation was less evident. H&E staining indicated that by 6 weeks, cellular proliferation of infiltrated cells was well established. At 6 weeks, these cells also began elaborating a collagen matrix that continued to mature and increase in the fractional area through week 12.

The extent of collagen deposition was different between IA and bone tunnel regions of the graft. Cells in the bone tunnel region began elaborating a collagen earlier than those in the IA region, as evidenced by a higher area fraction of
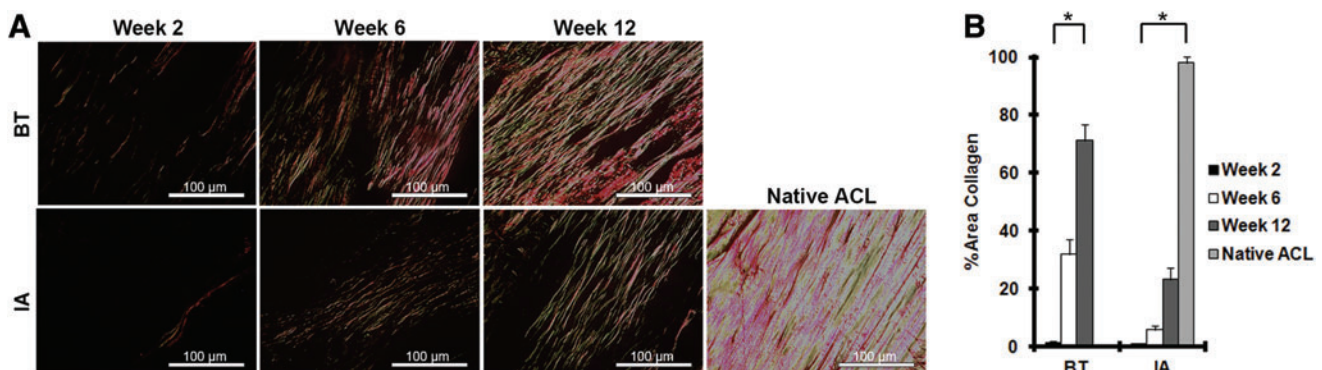
FIG. 7. Quantitative assessment of *in vivo* collagen deposition. **(A)** Representative images of Picrosirius red staining are depicted for IA and BT regions at weeks 2, 6, and 12 and show gradual increases in fibrillar collagen type I and type III deposition. **(B)** ImageJ was used to analyze the percentage of field of view containing birefringent pixels for each HPF analyzed ($n = 5$). *A p value of < 0.01 between all groups. Color images available online at www.liebertpub.com/tea

TABLE 1. HISTOLOGY GRADING SCORES FOR INTRA-ARTICULAR AND BONE TUNNEL REGIONS OF GRAFT ($N=4$)

	Grade[a] (points)					
	Cell morphology	Inflammatory response	Matrix staining intensity	Fibrocartilage formation	New bone formation	Graft bonding to bone
BT						
2 weeks	3, 4, 4, 4	0, 3, 2, 2	2, 1, 1, 2	0, 0, 0, 0	1, 2, 2, 2	2, 4, 2, 2
6 weeks	4, 4, 4, 3	4, 3, 2, 2	4, 3, 4, 3	2, 2, 4, 4	4, 2, 4, 5	4, 4, 4, 4
12 weeks	4, 4, 2, 3	2, 2, 3, 2	2, 2, 4, 3	4, 4, 3, 3	4, 3, 5, 5	4, 4, 5, 4
IA						
2 weeks	1, 0, 0, 1	0, 2, 2, 0	0, 2, 0, 0	N/A	N/A	N/A
6 weeks	1, 2, 2, 2	3, 4, 2, 3	2, 4, 2, 2	N/A	N/A	N/A
12 weeks	4, 6, 4, 2	2, 2, 4, 4	4, 5, 6, 2	N/A	N/A	N/A
Kappa	0.56	0.63	0.63	0.75	0.35	0.81

Histological grading of hematoxylin and eosin-stained slides to qualitatively assess scaffold integration into host tissue ($n=4$).

[a]Each section was graded by two independent observers from 0 to 3 to denote none, slight, moderate, or abundant. Sums of these two scores for each implanted animal were recorded (0–6) along with intraobserver agreement values (Cohen's Kappa coefficient) for each item, indicating fair (0.21–0.40), moderate (0.41–0.60), good (0.61–0.80), and excellent (0.81–1) agreement for all categories. Note that fibrocartilage formation, new bone formation, and graft bonding to bone are not applicable measures for IA graft regions.

BT, bone tunnel; IA, intra-articular.

collagen in the BT at the 2-week time point. This disparity in matrix deposition is likely due to the different vascularity in the BTs and in the joint space. Bone is well-vascularized, while the joint space is bathed in synovial fluid and contains limited vasculature, particularly in the region of the native ACL.[3] Matrix staining intensity and cellularity decreased gradually as a function of distance from the BT entrance site. The difference between BT and IA regions, however, became less apparent over time, suggesting that ligamentization may begin in the BT and progress toward the IA space. After 12 weeks *in vivo*, the implanted graft began to exhibit signs of matrix remodeling and aligned collagen deposition. Anisotropic collagen fibers were visible in Picrosirius red staining of both IA and bone tunnel regions of the graft at 12 weeks. These aligned collagen fibers are visually similar to the native ACL and suggest that the graft is progressing toward the appearance of native ligament. However, the collagen deposition and organization at 12 weeks still remain less than that demonstrated in the native rat ACL, indicating that further remodeling may be seen if the experiment was taken out to more extended time points.

Biomechanical analysis of the implanted PCL graft

Mechanical testing revealed that the mechanical properties of the implanted graft improved from time zero to the

TABLE 2. BIOMECHANICAL PROFILE OF POLYCAPROLACTONE ENGINEERED GRAFT AND NATIVE LIGAMENTS ($N=6$)

	Failure load (N)	Stiffness (N/mm)
Time zero implantation	3.95 ± 0.33	1.95 ± 0.35
12 weeks postimplantation	13.27 ± 4.20	15.98 ± 5.03
Native anterior cruciate ligament	35.45 ± 3.33	51.56 ± 9.70

Biomechanical profiles of polycaprolactone construct immediately following implantation (time zero), 12 weeks following implantation, and native anterior cruciate ligament.

12-week time point. Both load to failure and stiffness of the implanted graft increased over 12 weeks. The values of load to failure and stiffness obtained for the tissue-engineered graft were higher than the polymer scaffold tested immediately following implantation, but lower than the native ligament. This indicates that ligament regeneration has progressed over 12 weeks, but is insufficient to completely recapitulate the strength of the native ACL at that time. Again, further experiments with longer time points are necessary to determine whether the graft can further mature and remodel with mechanical properties similar to the native rat ACL.

Limitations of the study design

The current study has some weaknesses that warrant attention. While standalone PCL was tested in this current experiment, in the future, it may be useful to evaluate PCL copolymer blends, which may couple better initial mechanical properties with limited inflammatory response and satisfactory long-term matrix deposition. Moreover, this current experiment did not compare the polymeric graft to an autograft control tendon or ligament. Autograft collagen would likely have a less profound immunogenic response and would clearly have a more similar histologic appearance to the native ACL. Indeed, we contend that the native ACL is the ultimate control and we have compared our biomechanical findings to this standard.

Conclusions

This study employed an acellular electrospun PCL graft to reconstruct the rodent ACL and demonstrated the elaboration of collagen throughout the graft with a concurrent improvement of mechanical properties of the graft over time. In addition, we found that PCL elicits a minimal inflammatory response in the rodent model. Due to the biocompatibility and successful deposition of an aligned collagen matrix, future studies of electrospun PCL for ligament engineering models are warranted. In addition, the incorporation of growth factors and supporting cell types

could be used to enhance host integration and graft functioning, as well as the use of other copolymer blends.

Disclosure Statement

No competing financial interests exist.

References

1. Prodromos, C.C., Han, Y., Rogowski, J., Joyce, B., and Shi, K. A meta-analysis of the incidence of anterior cruciate ligament tears as a function of gender, sport, and a knee injury-reduction regimen. Arthroscopy **23,** 1320, 2007.

2. Klimkiewicz, J.J., Petrie, R.S., and Harner, C.D. Surgical treatment of combined injury to anterior cruciate ligament, posterior cruciate ligament, and medial structures. Clin Sport Med **19,** 479, 2000.

3. Petrigliano, F.A., McAllister, D.R., and Wu, B.M. Tissue engineering for anterior cruciate ligament reconstruction: a review of current strategies. Arthroscopy **22,** 441, 2006.

4. De Groot, J.H., de Vrijer, R., Pennings, A.J., Klompmaker, J., Veth, R.P., and Jansen, H.W. Use of porous polyurethanes for meniscal reconstruction and meniscal prostheses. Biomaterials **17,** 163, 1996.

5. Duling, R.R., Dupaix, R.B., Katsube, N., and Lannutti, J. Mechanical characterization of electrospun polycaprolactone (PCL): a potential scaffold for tissue engineering. J Biomech Eng **130,** 011006, 2008.

6. Woodruff, M.A., and Hutmacher, D.W. The return of a forgotten polymer—polycaprolactone in the 21st century. Prog Polym Sci **35,** 1217, 2010.

7. Nair, L.S., and Laurencin, C.T. Biodegradable polymers as biomaterials. Prog Polym Sci **32,** 762, 2007.

8. Lee, K.H., Kim, H.Y., Khil, M.S., Ra, Y.M., and Lee, D.R. Characterization of nano-structured poly(ε-caprolactone) nonwoven mats via electrospinning. Polymer **44,** 1287, 2003.

9. Hu, J.-Z., Zhou, Y.-C., Huang, L.-H., and Lu, H.-B. Development of biodegradable polycaprolactone film as an internal fixation material to enhance tendon repair: an *in vitro* study. BMC Musculoskelet Disord **14,** 246, 2013.

10. Pham, Q.P., Sharma, U., and Mikos, A.G. Electrospun poly (epsilon-caprolactone) microfiber and multilayer nanofiber/microfiber scaffolds: characterization of scaffolds and measurement of cellular infiltration. Biomacromolecules **7,** 2796, 2006.

11. Bölgen, N., Vargel, I., Korkusuz, P., Menceloğlu, Y.Z., and Pişkin, E. *In vivo* performance of antibiotic embedded electrospun PCL membranes for prevention of abdominal adhesions. J Biomed Mater Res B Appl Biomater **81,** 530, 2007.

12. Chung, A.S., Hwang, H.S., Das, D., Zuk, P., McAllister, D.R., and Wu, B.M. Lamellar stack formation and degradative behaviors of hydrolytically degraded poly(ε-caprolactone) and poly(glycolide-ε-caprolactone) blended fibers. J Biomed Mater Res B Appl Biomater **100,** 274, 2012.

13. Choi, J.S., Lee, S.J., Christ, G.J., Atala, A., and Yoo, J.J. The influence of electrospun aligned poly(ε-caprolactone)/

collagen nanofiber meshes on the formation of self-aligned skeletal muscle myotubes. Biomaterials **29,** 2899, 2008.

14. Shao, Z., Zhang, X., Pi, Y., Wang, X., Jia, Z., Zhu, J., *et al.* Polycaprolactone electrospun mesh conjugated with an MSC affinity peptide for MSC homing *in vivo*. Biomaterials **33,** 3375, 2012.

15. Tillman, B.W., Yazdani, S.K., Lee, S.J., Geary, R.L., Atala, A., and Yoo, J.J. The *in vivo* stability of electrospun polycaprolactone-collagen scaffolds in vascular reconstruction. Biomaterials **30,** 583, 2009.

16. Wise, S.G., Byrom, M.J., Waterhouse, A., Bannon, P.G., Weiss, A.S., and Ng, M.K.C. A multilayered synthetic human elastin/polycaprolactone hybrid vascular graft with tailored mechanical properties. Acta Biomater **7,** 295, 2011.

17. Cao, H., McHugh, K., Chew, S.Y., and Anderson, J.M. The topographical effect of electrospun nanofibrous scaffolds on the *in vivo* and *in vitro* foreign body reaction. J Biomed Mater Res A **93,** 1151, 2010.

18. Joshi, V.S., Lei, N.Y., Walthers, C.M., Wu, B., and Dunn, J.C.Y. Macroporosity enhances vascularization of electrospun scaffolds. J Surg Res **183,** 18, 2013.

19. Vaz, C.M., van Tuijl, S., Bouten, C.V.C., and Baaijens, F.P.T. Design of scaffolds for blood vessel tissue engineering using a multi-layering electrospinning technique. Acta Biomater **1,** 575, 2005.

20. Lin, V.S., Lee, M.C., O'Neal, S., McKean, J., and Sung, K.L. Ligament tissue engineering using synthetic biodegradable fiber scaffolds. Tissue Eng **5,** 443, 1999.

21. An, J., Chua, C.K., Leong, K.F., Chen, C.-H., and Chen, J.-P. Solvent-free fabrication of three dimensionally aligned polycaprolactone microfibers for engineering of anisotropic tissues. Biomed Microdevices **14,** 863, 2012.

22. Bedi, A., Kovacevic, D., Fox, A.J.S., Imhauser, C.W., Stasiak, M., Packer, J., *et al.* Effect of early and delayed mechanical loading on tendon-to-bone healing after anterior cruciate ligament reconstruction. J Bone Joint Surg Am **92,** 2387, 2010.

23. Kawamura, S., Ying, L., Kim, H.-J., Dynybil, C., and Rodeo, S.A. Macrophages accumulate in the early phase of tendon-bone healing. J Orthop Res **23,** 1425, 2005.

24. Fan, H., Liu, H., Wong, E.J.W., Toh, S.L., and Goh, J.C.H. *In vivo* study of anterior cruciate ligament regeneration using mesenchymal stem cells and silk scaffold. Biomaterials **29,** 3324, 2008.

25. Yeh, W.-L., Lin, S.-S., Yuan, L.-J., Lee, K.-F., Lee, M.Y., and Ueng, S.W.N. Effects of hyperbaric oxygen treatment on tendon graft and tendon-bone integration in bone tunnel: biochemical and histological analysis in rabbits. J Orthop Res **25,** 636, 2007.

26. Joshi, S.M., Mastrangelo, A.N., Magarian, E.M., Fleming, B.C., and Murray, M.M. Collagen-platelet composite enhances biomechanical and histologic healing of the porcine anterior cruciate ligament. Am J Sports Med **37,** 2401, 2009.

27. Landis, J.R., and Koch, G.G. The measurement of observer agreement for categorical data. Biometrics **33,** 159, 1977.

28. Bourke, S.L., Kohn, J., and Dunn, M.G. Preliminary development of a novel resorbable synthetic polymer fiber scaffold for anterior cruciate ligament reconstruction. Tissue Eng **10,** 43, 2004.

29. Fisher, M.B., Liang, R., Jung, H.-J., Kim, K.E., Zamarra, G., Almarza, A.J., *et al.* Potential of healing a transected anterior cruciate ligament with genetically modified extracellular matrix bioscaffolds in a goat model. Knee Surg Sports Traumatol Arthrosc **20,** 1357, 2012.

30. Ma, J., Smietana, M.J., Kostrominova, T.Y., Wojtys, E.M., Larkin, L.M., and Arruda, E.M. Three-dimensional engineered bone-ligament-bone constructs for anterior cruciate ligament replacement. Tissue Eng Part A **18,** 103, 2012.

31. Murray, M.M., Spindler, K.P., Abreu, E., Muller, J.A., Nedder, A., Kelly, M., *et al.* Collagen-platelet rich plasma hydrogel enhances primary repair of the porcine anterior cruciate ligament. J Orthop Res **25,** 81, 2007.

32. Murray, M.M., Spindler, K.P., Devin, C., Snyder, B.S., Muller, J., Takahashi, M., *et al.* Use of a collagen-platelet rich plasma scaffold to stimulate healing of a central defect in the canine ACL. J Orthop Res **24,** 820, 2006.

33. Robayo, L.M., Moulin, V.J., Tremblay, P., Cloutier, R., Lamontagne, J., Larkin, A.-M., *et al.* New ligament healing model based on tissue-engineered collagen scaffolds. Wound Repair Regen **19,** 38, 2011.

34. Seo, Y.-K., Yoon, H.-H., Song, K.-Y., Kwon, S.-Y., Lee, H.-S., Park, Y.-S., *et al.* Increase in cell migration and angiogenesis in a composite silk scaffold for tissue-engineered ligaments. J Orthop Res **27,** 495, 2009.

35. Shahab-Osterloh, S., Witte, F., Hoffmann, A., Winkel, A., Laggies, S., Neumann, B., *et al.* Mesenchymal stem cell-dependent formation of heterotopic tendon-bone insertions (osteotendinous junctions). Stem Cells **28,** 1590, 2010.

36. Spalazzi, J.P., Dagher, E., Doty, S.B., Guo, X.E., Rodeo, S.A., and Lu, H.H. *In vivo* evaluation of a multiphased scaffold designed for orthopaedic interface tissue engineering and soft tissue-to-bone integration. J Biomed Mater Res A **86,** 1, 2008.

37. Leong, N.L., Petrigliano, F.A., and McAllister, D.R. Current tissue engineering strategies in anterior cruciate ligament reconstruction. J Biomed Mater Res A **102,** 1614, 2013.

38. Dash, T.K., and Konkimalla, V.B. Poly-ε-caprolactone based formulations for drug delivery and tissue engineering: a review. J Control Release **158,** 15, 2012.

39. Yoshimoto, H., Shin, Y.M., Terai, H., and Vacanti, J.P. A biodegradable nanofiber scaffold by electrospinning and its potential for bone tissue engineering. Biomaterials **24,** 2077, 2003.

Address correspondence to:
Frank A. Petrigliano, MD
Department of Orthopaedic Surgery
David Geffen School of Medicine at UCLA
CHS 76-143 10833 Le Conte Avenue
Los Angeles, CA 90095

E-mail: fpetrigliano@mednet.ucla.edu